

Colour-tunable ultra-long organic phosphorescence of a single-component molecular crystal

Long Gu^{1,5}, Huifang Shi^{1,5}, Lifang Bian¹, Mingxing Gu¹, Kun Ling¹, Xuan Wang¹, Huili Ma¹, Suzhi Cai¹, Weihua Ning¹, Lishun Fu¹, He Wang¹, Shan Wang¹, Yaru Gao¹, Wei Yao¹, Fengwei Huo¹, Youtian Tao¹, Zhongfu An^{1*}, Xiaogang Liu^{2*} and Wei Huang^{1,3,4*}

Materials exhibiting long-lived, persistent luminescence in the visible spectrum are useful for applications in the display, information encryption and bioimaging sectors^{1–4}. Herein, we report the development of several organic phosphors that provide colour-tunable, ultra-long organic phosphorescence (UOP). The emission colour can be tuned by varying the excitation wavelength, allowing dynamic colour tuning from the violet to the green part of the visible spectrum. Our experimental data reveal that these organic phosphors can have an ultra-long lifetime of 2.45 s and a maximum phosphorescence efficiency of 31.2%. Furthermore, we demonstrate the applications of colour-tunable UOP for use in a multicolour display and visual sensing of ultraviolet light in the range from 300 to 360 nm. The findings open the opportunity for the development of smart luminescent materials and sensors with dynamically controlled phosphorescence.

Tunable emission colour empowers luminescent materials with superior performance in optoelectronic applications. For instance, multicolour-encoded microparticles can serve as information carriers for high-density, encrypted data storage, anti-counterfeiting and multiplexed bioassay^{5,6}. Three-dimensional volumetric display could be realized using pulse-duration-sensitive upconversion nanocrystals⁷. Polychromatic luminescent materials are ideal biomarkers for multiplexed bio-imaging⁸. To date, multicolour emission can be obtained by modulating the material's composition, phase and crystallinity^{9–11}. Despite the success in realizing multicolour emission in luminescent materials^{12–14}, it remains a formidable challenge to develop a single-component molecular crystal that could exhibit dynamic colour tunability in response to variations in external physical parameters such as optical output, magnetic field, pressure and electric current.

Persistent luminescence with a long-lived emission lifetime is a fascinating optical phenomenon that has received considerable attention in photonics, organic electronics and bio-electronics. However, this phenomenon is mainly limited to inorganic materials based on transition metals and rare-earth ions¹⁵. Given harsh preparation conditions and the scarcity of metal resource components, special attention has recently been paid to metal-free organics with ultra-long organic phosphorescence (UOP)^{16–31}. Over the past few years, an extensive collection of persistent phosphors with colourful UOP have been developed at room temperature on the basis of different molecular skeletons and stacking motifs through

crystallization^{18–22}, host-guest doping²³, metal-organic framework (MOF) construction²⁴, H-aggregation^{25,26} and many others^{27–31}. To the best of our knowledge, researchers have yet to find a single-component material, in the form of inorganic phosphors or organic materials, with tunable persistent luminescence.

Notably, multicolour emission can be obtained in carbon dots under different excitations due to the formation of multiple emitting centres (Fig. 1a)³². Under cryogenic conditions, strong molecular phosphorescence with long-lived emission lifetimes can be observed from metal-free organic molecules in a dilute solution, due to the suppression of nonradiative transition through the efficient confinement of molecular motion at an atomic level³³. Inspired by multi-emitting centres for tunable colour emission in the carbon dots and high-efficiency molecular phosphorescence in cryogenic conditions, we speculate that the realization of tunable persistent luminescence is possible under different excitations by constructing multiple UOP emitting centres in a single-component molecular crystal under ambient conditions. Similar to the case of an emitter present in a cryogenic solution, a molecular emitter may be constructed by regulating in-plane intermolecular interactions through molecular engineering (Fig. 1b, left). Recently, we have developed a strategy to stabilize the triplet excited states for ultra-long phosphorescence by forming H-aggregation in single crystals (Fig. 1b, right)²⁵, which can serve as a phosphorescence emitting centre. We reason that, with a proper design, such molecular engineering can provide a versatile platform with a multicolour fine-tuning capability (Fig. 1c).

To validate our hypothesis, we designed a series of triazine derivatives containing multiple hetero atoms, which can not only improve the rate of intersystem crossing (ISC) to boost triplet excitons but also construct multiple intermolecular interactions to restrict molecular motion for molecular phosphorescence in solid states. In addition, molecules featuring planar configurations should promote the formation of H-aggregation, which stabilizes the excited triplet states in favour of UOP. As a proof of concept, we synthesized 2,4,6-trimethoxy-1,3,5-triazine (TMOT) and characterized this molecule by ¹H and ¹³C NMR spectroscopies, elemental analysis, single-crystal X-ray diffraction and photophysical properties (Supplementary Sections 1 and 2). As anticipated, long-lived green luminescence was observed from the TMOT crystalline powder under ambient conditions after the removal of the 365 nm ultraviolet (UV) lamp (Supplementary Fig. 17 and Supplementary Video 1).

¹Key Laboratory of Flexible Electronics & Institute of Advanced Materials, Nanjing Tech University, Nanjing, China. ²Department of Chemistry, National University of Singapore, Singapore, Singapore. ³Institute of Flexible Electronics, Northwestern Polytechnical University, Xi'an, China. ⁴Key Laboratory for Organic Electronics and Information Displays & Jiangsu Key Laboratory for Biosensors, Institute of Advanced Materials, Jiangsu National Synergetic Innovation Center for Advanced Materials, Nanjing University of Posts and Telecommunications, Nanjing, China. ⁵These authors contributed equally: Long Gu, Huifang Shi. *e-mail: iamzfan@njtech.edu.cn; chmlx@nus.edu.sg; iamwhuang@nwpu.edu.cn

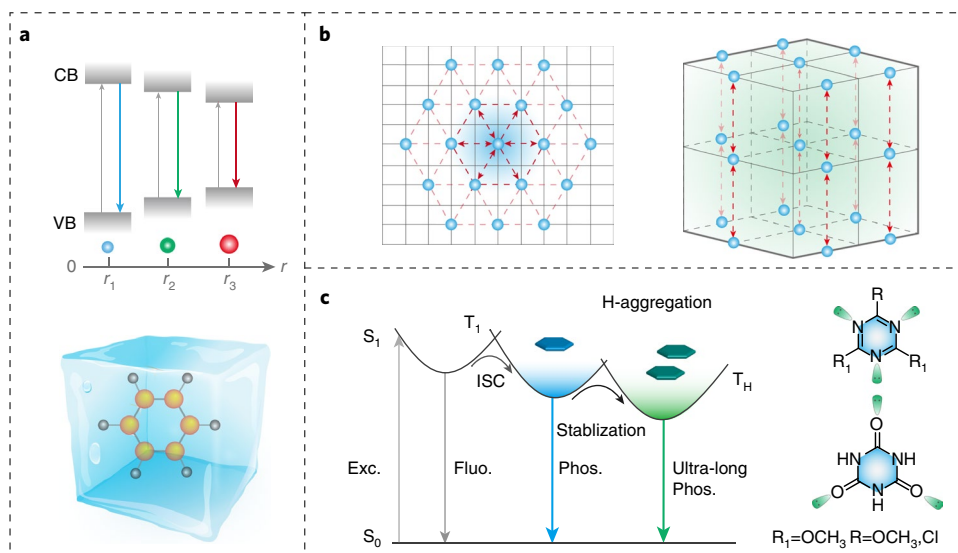


Fig. 1 | Schematic representation for the manipulation of colour-tunable UOP. **a**, Proposed mechanism of excitation-dependent multicolour luminescence in carbon dots (top) and an illustration of freezing molecules to boost molecular phosphorescence under cryogenic conditions (bottom). **b**, Top and lateral views of molecular packing in crystals. The red dashed lines and blue balls represent intermolecular interactions and the molecular phosphors, respectively. Each molecule was restricted by surrounding molecules with multiple intermolecular interactions in the same plane to suppress the molecular motion for molecular phosphorescence. UOP was obtained on the formation of H-aggregation by strong interlayer interactions. **c**, Proposed mechanism and molecular design for excitation-dependent colour-tunable UOP. The triplet excitons are generated from the singlet excitons through the intersystem crossing, enabling molecular phosphorescence owing to the strict suppression of the molecular motion in the same plane. The formation of H-aggregation can stabilize the triplet excitons and lead to aggregated phosphorescence. VB, valence band; CB, conduction band; r , radius; Exc., excitation; Fluor., fluorescence; Phos., phosphorescence.

The long-lived luminescence turned to a sky-blue colour as the excitation wavelength changed from 365 to 310 nm (Supplementary Fig. 17 and Supplementary Video 2), demonstrating the excitation-dependent nature of the long-lived luminescence.

We further attempted to measure the excitation–phosphorescence spectra of the TMOT crystalline powder under ambient conditions. As shown in Fig. 2a, with a change in the excitation wavelength from 250 to 400 nm, the long-lived luminescence exhibited an obvious bathochromic shift from sky-blue to green along with a variation in the main peak from 452 to 505 nm. Resolved phosphorescence spectra were simultaneously demonstrated (Supplementary Fig. 18). The colour variations of the TMOT powder in response to different excitation wavelengths are shown in the Commission International de l’Eclairage (CIE) coordinate diagram in Fig. 2b. As the excitation wavelength was gradually changed from 300 to 360 nm, the UOP changed from a blue to green colour with good linearity of the CIE coordinates (Fig. 2b). In addition, the TMOT powder exhibits the same excitation-dependent phosphorescence features under oxygen and nitrogen atmospheres at room temperature (Supplementary Figs. 19 and 20).

From the analysis of time-resolved emission spectra (Fig. 2c and Supplementary Table 1), it was found that the long-lived luminescence of the TMOT powder showed remarkably long lifetimes of 0.58 and 0.75 s following excitation at 320 and 365 nm, respectively, under ambient conditions (Supplementary Fig. 21). Notably, the maximum phosphorescence efficiency of the TMOT powder is about 31.2% (Supplementary Table 2), which is among the best results reported so far. As shown in Fig. 2d, with an enhanced excitation intensity on increasing the iris aperture from 10% to 100%, the UOP increased linearly after irradiation with different excitation wavelengths (Supplementary Fig. 22). An efficient multicolour ultra-long phosphorescence can be obtained for TMOT powder within a short period of excitation (<2 s) (Fig. 2e and Supplementary Fig. 23). From Fig. 2f, it is revealed that the

long-lived luminescence can be efficiently excited by UV light ranging from 250 to 390 nm. When the TMOT powder was excited by UV light from 250 to 347 nm, the blue luminescence was more intense than the green emission, whereas the luminescence of the sample was dominated by the green emission with excitation in the range from 347 to 390 nm. The ratiometric change in the emission intensities of 465 and 505 nm as a function of the excitation wavelength leads to colour-tunable phosphorescence.

To gain a deeper insight into the unique optical properties, we further conducted a set of control experiments, single-crystal X-ray diffraction analysis and theoretical calculations on the TMOT molecule. The phosphorescent property of TMOT was first investigated in a dilute solution of 2-methyltetrahydrofuran (m-THF) and in polymethyl methacrylate (PMMA)-encapsulated films (1, 5 and 10 wt. %) at 77 K. As shown in Fig. 3a and Supplementary Fig. 24, the TMOT molecule exhibited a broad blue emission band at around 445 nm only when excited at 320 nm, closely resembling the UOP (452 nm) occurring in single crystals. The lifetimes of the emission bands at around 445 nm for the TMOT molecule reached as much as 1.67 and 2.17 s in dilute solution and PMMA film at 77 K, respectively (Supplementary Fig. 25 and Supplementary Table 3). In addition, no green phosphorescence at around 505 nm was detectable, either in the solution or PMMA film, after irradiation at 320 or 365 nm. Therefore, the blue ultra-long luminescence can be ascribed to the phosphorescence of isolated molecules, like that observed in the solution or PMMA film, and the fact that green UOP was observed only in the solid form may stem from intermolecular aggregation. In the TMOT single crystal, each TMOT molecule was tethered by six adjacent molecules with multiple intermolecular interactions (C–H•••N) with distances of 2.757, 2.684 and 2.643 Å in the same plane (Fig. 3b), which could significantly limit molecular movement and suppress the nonradiative transition of triplet excitons in the crystalline state. The restriction of molecular movement at a single molecular level endowed the isolated molecule with

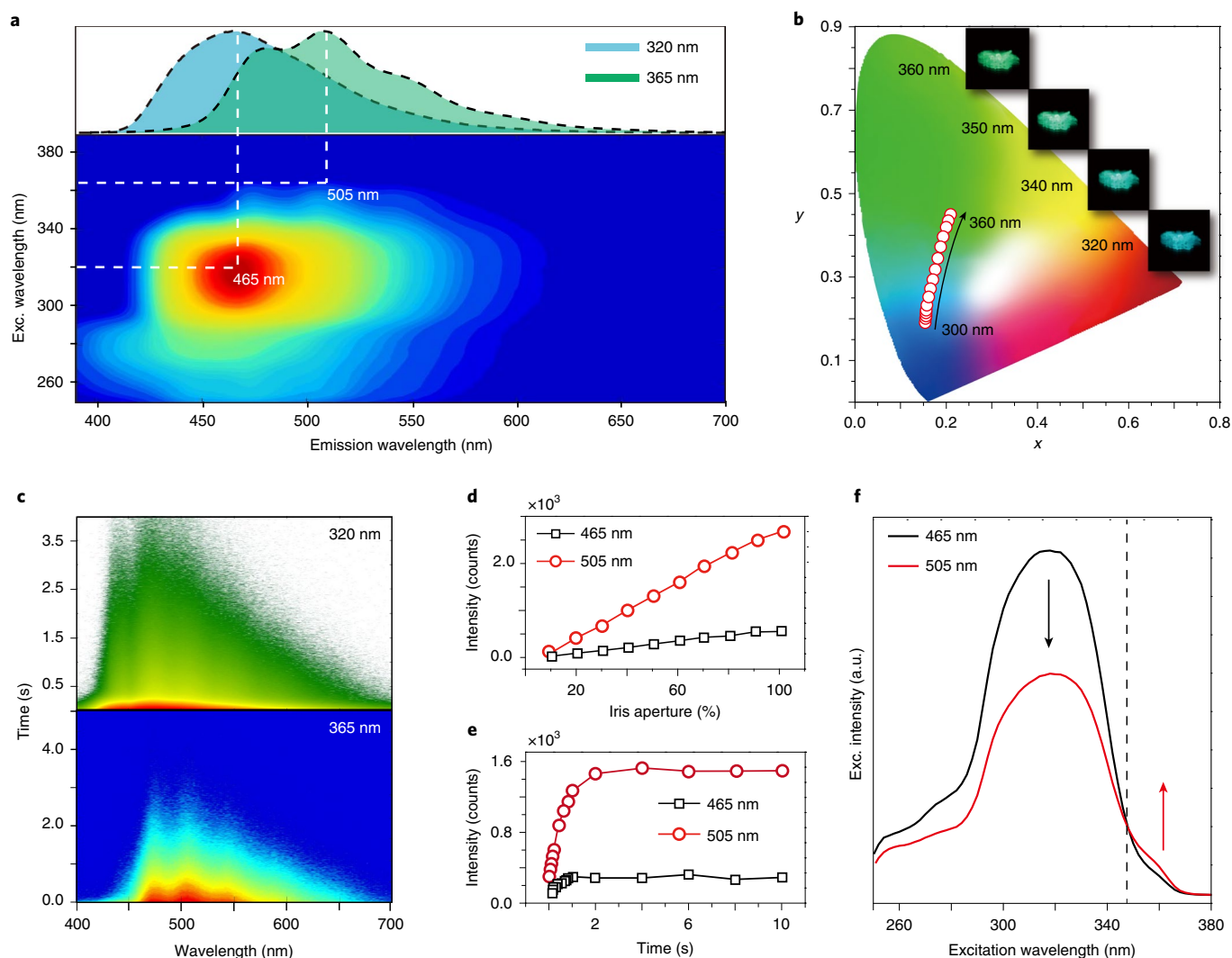


Fig. 2 | Photoluminescence characterization of TMOT crystalline powder under ambient conditions. **a**, Excitation–phosphorescence mapping of TMOT powder at 300 K. The upper inset shows the UOP spectra of the TMOT powder following excitation at 320 nm (blue) and 365 nm (green), respectively. **b**, Trajectory of colour modulation, recorded by the change in the excitation from 300 to 360 nm, in the CIE coordinate diagram. The inset images show the long-lived luminescence photographs of the TMOT powder taken following excitation at 320, 340, 350 and 360 nm, respectively. **c**, Transient photoluminescence decay images of the sample following excitation at 320 (top) and 365 nm (bottom), respectively. **d, e**, Corresponding intensities of the phosphorescence of the TMOT powder at 465 and 505 nm, obtained with varying excitation intensity (**d**) and excitation time (**e**). **f**, Excitation spectra of the TMOT molecules at 465 (black line) and 505 nm (red line), respectively. a.u., arbitrary units.

blue phosphorescence. The side view of the TMOT crystal structure showed face-to-face parallel arrangements with an H-aggregation feature through an intensive $\pi\cdots\pi$ interaction (3.348 Å), providing a possibility to stabilize the triplet excitons for green UOP (Fig. 3b).

Our speculation regarding unique UOP in TMOT was further verified by simulations (Supplementary Figs. 26–29). In monomeric and dimeric states, the lowest excited triplet states (T_1) were calculated to be 459 and 475 nm (Fig. 3c), respectively, which agree well with the experimental data for 452 and 481 nm (Supplementary Fig. 30). After the replacement of the methoxy group in the TMOT molecule by a phenyl, there existed only yellow-green UOP due to H-aggregation (Supplementary Fig. 31 and Supplementary Section 4). Notably, compared with the molecular packing in the TMOT crystal, the intermolecular interaction in the 2,6-methoxy-4-diphenyl-1,3,5-triazine (MOPT) crystal was weaker in restricting molecular motion in a plane (Fig. 3d). Therefore, we reason that strong intermolecular interactions along the same plane play a central role in realizing molecular phosphorescence. Taken together, we

speculate that with the change in excitation wavelength, a mixing of different ratios between molecular phosphorescence, restricted by intermolecular interactions in the same plane, and H-aggregation-mediated ultralong phosphorescence can result in tunable long-lived luminescence in single-component molecular crystals (Fig. 3e).

We further tested our hypothesis using two additional compounds, namely 2-chloro-4,6-dimethoxy-1,3,5-triazine (DMOT) and 1,3,5-triazine-2,4,6-trione (CYAD) (Supplementary Sections 1 and 4). Both DMOT and CYAD crystalline powders showed tunable ultra-long phosphorescence from violet to sky-blue by varying the excitation wavelength from 250 to 400 nm (Fig. 4a–d and Supplementary Figs. 37–39). For DMOT, the luminescence is centred at 430 nm with a lifetime of 2.45 s (Fig. 4e and Supplementary Table 1). For CYAD, the luminescence peak blue-shifted to 380 nm with a lifetime of 0.45 s (Fig. 4e). As shown in Fig. 4f,g, the long-lived luminescence can be efficiently excited by UV light ranging from 250 to 390 nm. Like TMOT, the excitation at different wavelengths can lead to a ratiometric variation between the molecular phosphorescence

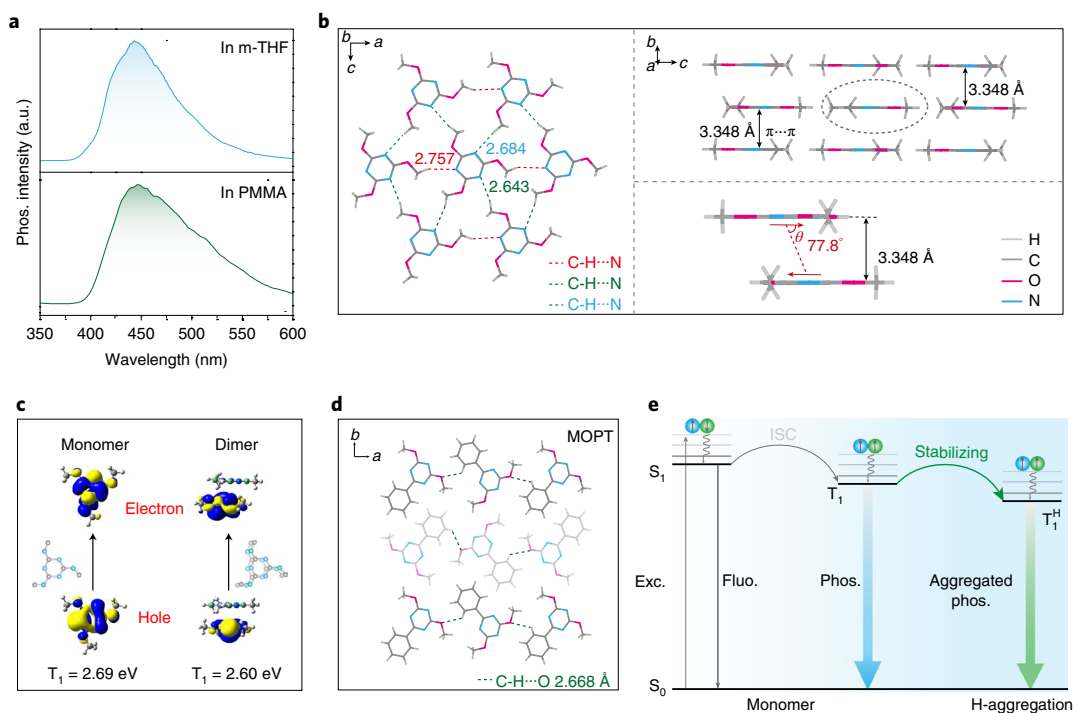


Fig. 3 | Mechanistic investigation of colour-tunable UOP in single-component crystals under ambient conditions. a, Normalized phosphorescence spectra of TMOT molecules in m-THF and PMMA film, recorded following excitation at 320 nm and 77 K. **b**, Molecular arrangement of the TMOT single crystal viewed along the *b* axis (left). The central molecule is stabilized by three types of intermolecular interactions through adjacent molecules. Molecular packing along the *a* axis (top right). Modelling of a TMOT dimer with the H-aggregation feature (bottom right). **c**, Natural transition orbitals (NTOs) contributing to the lowest-energy triplet transitions of a TMOT monomer and a dimer in the single crystal. **d**, Molecular packing of a control molecule, MOPT, viewed along the *c* axis. **e**, Proposed energy transfer processes of fluorescence (Fluo.), molecular phosphorescence (Phos.) and aggregated phosphorescence (Aggregated phos.) occurring in the TMOT crystal following excitation (Exc.).

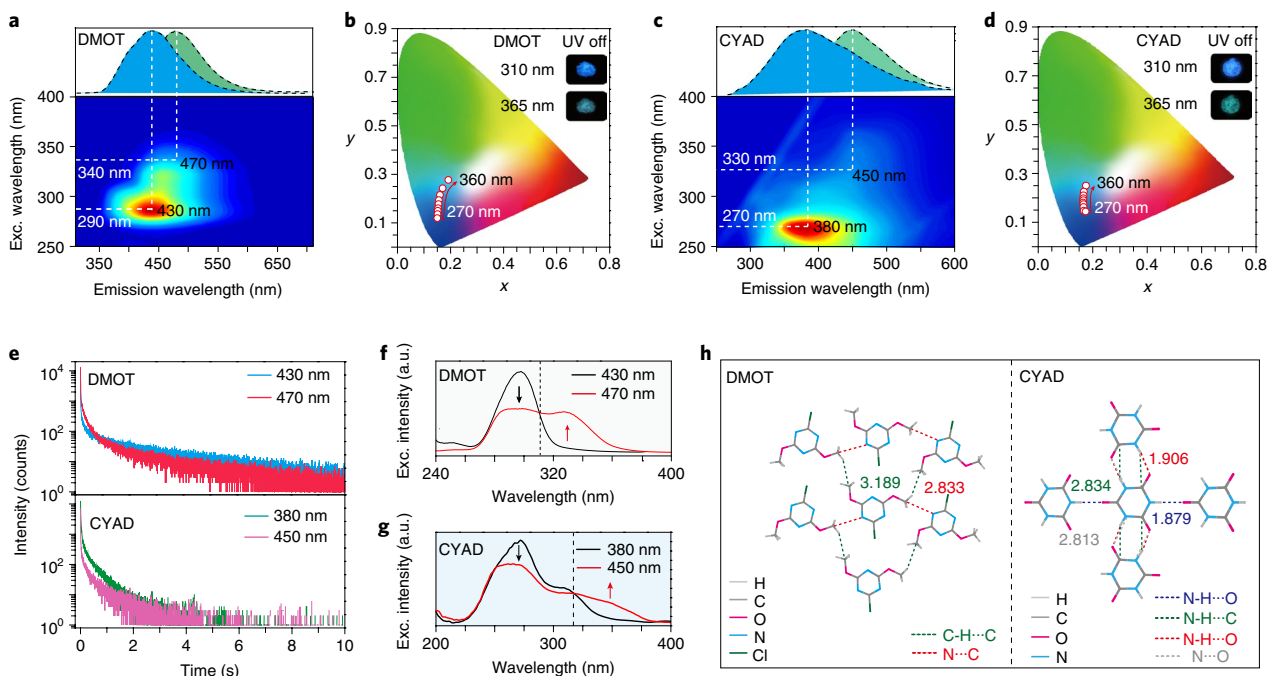


Fig. 4 | Phosphorescence properties and crystal structures of DMOT and CYAD crystalline powder under ambient conditions. a, c, Excitation-phosphorescence mapping of DMOT and CYAD. The upper inset shows the phosphorescence spectra of DMOT and CYAD molecules, recorded under excitation at different wavelengths. **b, d**, Trajectory of tunable UOP emission colours, recorded on changing the excitation wavelength of DMOT and CYAD from 270 to 360 nm in the CIE coordinate diagram. Inset: photographs taken after the removal of 310 and 365 nm excitation, respectively. **e**, Lifetime profiles of emission bands at 430 and 470 nm for DMOT and at 380 and 450 nm for CYAD, respectively. **f, g**, Excitation spectra obtained by monitoring the emission at 430 and 470 nm for DMOT and at 380 and 450 nm for CYAD, respectively. **h**, Top-view crystal structures of DMOT and CYAD showing detailed information on the intermolecular interactions. The dashed lines represent intermolecular interactions.

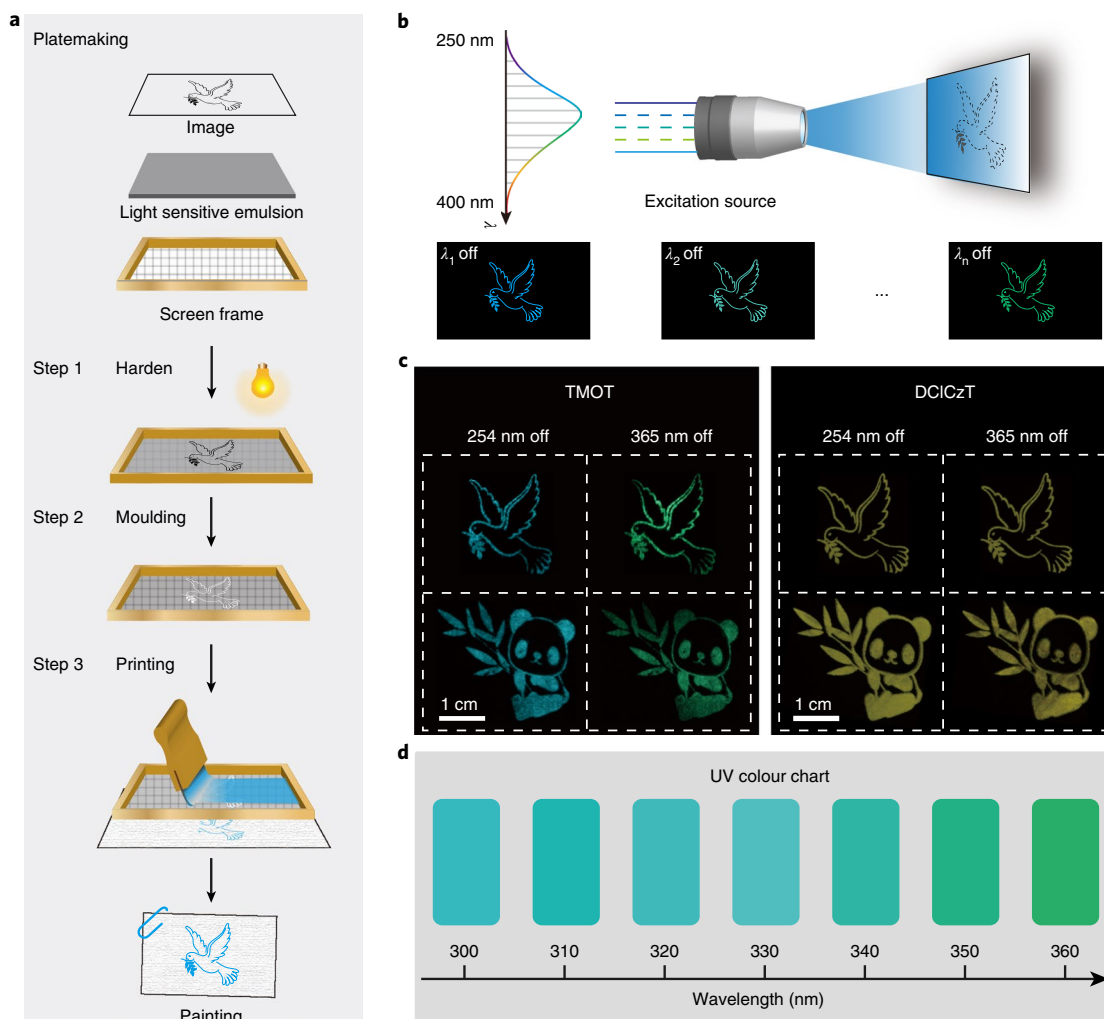


Fig. 5 | Demonstration of colour-tunable UOP for multicolour display and visual detection of ultraviolet light under ambient conditions. **a**, Screen printing process adopted for patterning. A small amount of the emulsion was painted with a squeegee onto a screen, on which a transparent, pre-designed image was laid afterwards. On completely drying and hardening through the use of a lamp, the screen was laid over a filter paper and an ink containing phosphorescent materials was printed onto the screen to generate a painting. **b**, Schematic of the experimental set-up for multicolour display by varying the excitation wavelength from 250 to 400 nm. **c**, The UOP photographs of peace dove and panda patterns, recorded with the TMOT (left) and DCICzT (right) as the ink, respectively. Note that the phosphorescence images were recorded after switching off a 254 or 365 nm hand-held UV lamp. **d**, UV colour chart showing the ability of using TMOT crystalline powder to visually detect specific wavelengths in the UV region.

and ultra-long phosphorescence from aggregations in DMOT and CYAD crystalline powder, possibly resulting in colour-tunable ultra-long organic phosphorescence in single-component crystals. In addition to H-aggregation (Supplementary Fig. 31), molecules in the same plane were strictly restricted through the multiple intermolecular interactions shown (Fig. 4h and Supplementary Section 5). Remarkably, the percentage of restricted atoms in the CYAD molecule was up to 75% (Supplementary Fig. 44).

On the basis of the excitation-dependent UOP feature of the newly developed single-component phosphors, we took one step further to demonstrate their potential applications for multicolour display and visual detection of a specific wavelength in the UV region. Different patterns, such as a peace dove, a panda, Cp rings, and a butterfly, with different sizes from 1 to 3.5 cm were fabricated through a simple silk-screen printing technique by grinding TMOT and 9-(4,6-dichloro-1,3,5-triazin-2-yl)-9H-carbazole (DCICzT) powder as a solid ink (Fig. 5a and Supplementary Section 6). On changing the excitation wavelength from 254 to 365 nm, the phosphorescence image turned from sky-blue to green (Fig. 5b).

By comparison, the control phosphorescence imaging of DCICzT showed a constant yellow colour, independent of the excitation wavelength (Fig. 5c and Supplementary Fig. 47). Interestingly, as the invisible UV excitation changed from 300 to 360 nm with an interval of 10 nm, colourful, visual phosphorescence images could be captured by the naked eye (Fig. 5d and Supplementary Fig. 48), demonstrating its potential utility for the detection of UV light. The specific wavelength of the UV light can be precisely identified by correlating the excitation wavelength and the CIE chromaticity coordinates (Supplementary Fig. 49). It is worth noting that a low power of UV irradiation at $10 \mu\text{W cm}^{-2}$ is detectable (Supplementary Fig. 50).

In conclusion, we have reported the development of a series of organic molecules featuring colour-tunable ultra-long organic phosphorescence in single-component molecular crystals. On changing the excitation wavelength, the emission colours of these organic molecules can be dynamically tuned from the violet (380 nm) to green (505 nm) under ambient conditions. In light of both the experimental results and simulation, we believe that mitigation

of molecular movement in the same plane and H-aggregation are responsible for the tunable UOP under study. By tailoring the structure of such molecules, the lifetime and phosphorescence quantum efficiency of phosphors can reach values up to 2.45 s and 31.2%, respectively, under ambient conditions. Importantly, our investigation not only provides a fundamental design principle for realizing colour-tunable UOP in single-component molecular crystals, but also offers an opportunity for developing a convenient platform for multiplexed biological labelling, multicolour displays, anti-counterfeiting, UV detection, and potentially many others.

Online content

Any methods, additional references, Nature Research reporting summaries, source data, statements of data availability and associated accession codes are available at <https://doi.org/10.1038/s41566-019-0408-4>.

Data availability

The data that support the plots within this paper and other findings of this study are available from the corresponding author upon reasonable request.

Received: 24 November 2018; Accepted: 26 February 2019;

Published online: 8 April 2019

References

- Pan, Z., Lu, Y. & Liu, F. Sunlight-activated long-persistent luminescence in the near-infrared from Cr³⁺-doped zinc gallogermanates. *Nat. Mater.* **11**, 58–63 (2012).
- Maldiney, T. et al. The in vivo activation of persistent nanophosphors for optical imaging of vascularization, tumours and grafted cells. *Nat. Mater.* **13**, 418–426 (2014).
- Xu, S., Chen, R., Zheng, C. & Huang, W. Excited state modulation for organic afterglow: materials and applications. *Adv. Mater.* **28**, 9920–9940 (2016).
- Su, Y. et al. Ultralong room temperature phosphorescence from amorphous organic materials toward confidential information encryption and decryption. *Sci. Adv.* **4**, 9732–9743 (2018).
- Lee, J. et al. Universal process-inert encoding architecture for polymer microparticles. *Nat. Mater.* **13**, 524–529 (2014).
- Lee, H., Kim, J., Kim, H., Kim, J. & Kwon, S. Colour-barcode magnetic microparticles for multiplexed bioassays. *Nat. Mater.* **9**, 745–749 (2010).
- Deng, R. et al. Temporal full-colour tuning through non-steady-state upconversion. *Nat. Nanotechnol.* **10**, 237–242 (2015).
- Pan, L. et al. Truly fluorescent excitation-dependent carbon dots and their applications in multicolor cellular imaging and multidimensional sensing. *Adv. Mater.* **27**, 7782–7787 (2015).
- Farinola, G. M. & Ragni, R. Electroluminescent materials for white organic light emitting diodes. *Chem. Soc. Rev.* **40**, 3467–3482 (2011).
- Irie, M., Fukaminato, T., Matsuda, K. & Kobatake, E. Photochromism of diarylethene molecules and crystals: memories, switches, and actuators. *Chem. Rev.* **114**, 12174–12277 (2014).
- Mao, Z. et al. Linearly tunable emission colors obtained from a fluorescent-phosphorescent dual-emission compound by mechanical stimuli. *Angew. Chem. Int. Ed.* **54**, 6270–6273 (2015).
- Sun, Y. et al. Quantum-sized carbon dots for bright and colorful photoluminescence. *J. Am. Chem. Soc.* **128**, 7756–7757 (2006).
- Chen, O. et al. Excitation-intensity-dependent color-tunable dual emissions from manganese-doped CdS/ZnS core/shell nanocrystals. *Angew. Chem. Int. Ed.* **49**, 10132–10135 (2010).
- Lee, K. et al. Excitation-dependent visible fluorescence in decameric nanoparticles with monoacylglycerol cluster chromophores. *Nat. Commun.* **4**, 1544–1551 (2013).
- Xu, J. & Tanabe, S. Persistent luminescence instead of phosphorescence: History, mechanism, and perspective. *J. Lumin.* **205**, 581–620 (2019).
- Bolton, O., Lee, K., Kim, H., Lin, K. Y. & Kim, J. Activating efficient phosphorescence from purely organic materials by crystal design. *Nat. Chem.* **3**, 205–210 (2011).
- Zhang, G. et al. Multi-emissive difluoroboron dibenzoylmethane polylactide exhibiting intense fluorescence and oxygen-sensitive room-temperature phosphorescence. *J. Am. Chem. Soc.* **129**, 8942–8943 (2007).
- Yang, Z. et al. Intermolecular electronic coupling of organic units for efficient persistent room-temperature phosphorescence. *Angew. Chem. Int. Ed.* **55**, 2181–2185 (2016).
- He, Z. et al. White light emission from a single organic molecule with dual phosphorescence at room temperature. *Nat. Commun.* **8**, 416 (2017).
- Xie, Y. et al. How the molecular packing affects the room temperature phosphorescence in pure organic compounds: ingenious molecular design, detailed crystal analysis, and rational theoretical calculations. *Adv. Mater.* **29**, 1606829–1606836 (2017).
- Shoji, Y. et al. Unveiling a new aspect of simple arylboronic esters: long-lived room-temperature phosphorescence from heavy-atom-free molecules. *J. Am. Chem. Soc.* **139**, 2728–2733 (2017).
- Wei, J. et al. Induction of strong long-lived room-temperature phosphorescence of N-phenyl-2-naphthylamine molecules by confinement in a crystalline dibromobiphenyl matrix. *Angew. Chem. Int. Ed.* **55**, 15589–15593 (2016).
- Hirata, S. et al. Efficient persistent room temperature phosphorescence in organic amorphous materials under ambient conditions. *Adv. Funct. Mater.* **23**, 3386–3397 (2013).
- Yang, X. & Yan, D. Strongly enhanced long-lived persistent room temperature phosphorescence based on the formation of metal-organic hybrids. *Adv. Opt. Mater.* **4**, 897–905 (2016).
- An, Z. et al. Stabilizing triplet excited states for ultralong organic phosphorescence. *Nat. Mater.* **14**, 685–690 (2015).
- Lucenti, E. et al. Cyclic triimidazole derivatives: intriguing examples of multiple emissions and ultralong phosphorescence at room temperature. *Angew. Chem. Int. Ed.* **56**, 16302–16307 (2017).
- Ma, X., Xu, C., Wang, J. & Tian, H. Heavy-atom-free amorphous pure organic polymers with efficient room-temperature phosphorescence emission. *Angew. Chem. Int. Ed.* **130**, 11020–11024 (2018).
- Li, Q. et al. Induction of long-lived room temperature phosphorescence of carbon dots by water in hydrogen-bonded matrices. *Nat. Commun.* **9**, 734 (2018).
- Dou, X. et al. Clustering-triggered emission and persistent room temperature phosphorescence of sodium alginate. *Biomacromolecules* **19**, 2014–2022 (2018).
- Ogoshi, T. et al. Ultralong room-temperature phosphorescence from amorphous polymer poly(styrene sulfonic acid) in air in the dry solid state. *Adv. Funct. Mater.* **28**, 1707369–1707376 (2018).
- Tao, S. et al. Design of metal-free polymer carbon dots: a new class of room temperature phosphorescent materials. *Angew. Chem. Int. Ed.* **57**, 2393–2398 (2018).
- Kim, T. et al. Full-colour quantum dot displays fabricated by transfer printing. *Nat. Photon.* **5**, 176–182 (2011).
- Baryshnikov, G., Minaev, B. & Ågren, H. Theory and calculation of the phosphorescence phenomenon. *Chem. Rev.* **117**, 6500–6537 (2017).

Acknowledgements

This work is supported by the National Natural Science Foundation of China (21875104, 51673095, 91833304, 91833302 and 61605074), National Basic Research Program of China (973 Program, No. 2015CB932200), Natural Science Fund for Distinguished Young Scholars of Jiangsu Province (BK20180037), the Natural Science Fund for Colleges and Universities (17KJB430020) of Jiangsu Province, and Nanjing Tech Start-up Grant (3983500158 and 3983500169). We are grateful to the High Performance Computing Center of Nanjing Tech University for technical support.

Author contributions

L.G., H.S., Z.A., X.L. and W.H. conceived the experiments. H.S., Z.A., X.L. and W.H. wrote the manuscript. L.G., H.S., L.B., M.G., S.W., Y.G., W.Y. and F.H. were primarily responsible for the experiments. K.L. and L.F. measured the quantum efficiency. X.W., S.W. and H.W. performed the lifetime measurements. S.C., W.N. and Y.T. conducted the single-crystal measurement and analysis. H.M. contributed to TD-DFT calculations. All authors contributed to the data analyses.

Competing interests

The authors declare no competing interests.

Additional information

Supplementary information is available for this paper at <https://doi.org/10.1038/s41566-019-0408-4>.

Reprints and permissions information is available at www.nature.com/reprints.

Correspondence and requests for materials should be addressed to Z.A., X.L. or W.H.

Publisher's note: Springer Nature remains neutral with regard to jurisdictional claims in published maps and institutional affiliations.

© The Author(s), under exclusive licence to Springer Nature Limited 2019